ELSEVIER

Journal of Alloys and Compounds 293–295 (1999) 185–189

Journal of ALLOYS AND COMPOUNDS

Systematic B-metal substitution in $CaNi_5$

J.O. Jensen*, N.J. Bjerrum

Department of Chemistry, Building 207, Technical University of Denmark, DK-2800 Lyngby, Denmark

Abstract

The aim of this work has been to study the effect of B metal substitutions in $CaNi_5$ (AB_5) which is known to suffer from poor cycling stability as a hydride electrode material. Systematic monosubstitutions of nickel with the most common other B metals (i.e. Al, Cr, Mn, Fe, Co, Cu, Zn and Sn) and Mg were performed. The overall composition was in all cases $CaNi_{5-x}M_x$ ($x=0.5$ or 1) where M is the substituting element. The alloys were prepared by mechanical alloying. The hydrogen storage capacity was measured electrochemically ranging from 39 to 390 mAh/g, but none of the substitutions increased the cycling stability to any significant extend compared to pure $CaNi_5$. X-ray diffraction patterns of the alloys revealed that only in a few cases the hexagonal $CaCu_5$ structure of a true AB_5 alloy was preserved. In most cases diffraction patterns matching Ca_2Ni_7, $CaNi_3$ or $CaNi_2$ were seen. It can be concluded that $CaNi_5$ is much less tolerant towards B-metal substitution than $LaNi_5$. This fact makes it less possible that the problem with cycling stability of Ca-based hydride electrodes can be solved by substitutions.

Keywords: Hydrides; $CaNi_5$; Electrodes; Substitution; Hydrogen storage

1. Introduction

The far most successful hydride forming alloys for battery purposes belong to the AB_5 class developed from $LaNi_5$ with hexagonal $CaCu_5$ structure. In the search for cheaper materials with high capacity only little attention has been paid to the iso-structural calcium system exemplified by $CaNi_5$. $CaNi_5$ has an electrode capacity close to 400 mAh/g but a poor cycling stability. Apart from $CaNi_5$ the calcium nickel phase diagram comprises the compounds Ca_2Ni_7, $CaNi_3$ and $CaNi_2$ [1]. A description of $CaNi_5$ and $CaNi_5H_x$ with PC isotherms is given by Sandrock et al. [2].

The cycling stability of $LaNi_5$ has been improved dramatically by multiple substitutions resulting in the present mischmetal (Mm) alloys like $MmNi_{3.6}Co_{0.7}Mn_{0.4}Al_{0.3}$. Substitutions in $CaNi_5$ are only reported in a few cases. In this work calcium based alloys were prepared with systematic monosubstitutions of nickel with the most common B metals (i.e. Al, Cr, Mn, Fe, Co, Cu, Zn and Sn) and Mg. The overall composition was in all cases $CaNi_{5-x}M_x$ ($x=0.5$ or 1) where M is the substituting element.

2. Experimental

The alloys were prepared by mechanical alloying in a planetary ball mill (Fritsch Pulverisette 7) with vials and balls of steel. Freshly made calcium filings were added to the vials together with the alloying metals in the form of powder, granules or pieces of wire. After 4 h of premilling the samples were scraped off the vials and milled for additional 4 h. The alloys were then annealed for 12 h at 700°C in argon in sealed steel containers. This whole alloying technique was previously developed for the preparation of $CaNi_5$ without substitutions [3].

The alloys were subjected to X-ray powder diffraction in a Philips PW 1729-1820-1710 powder diffractometer with Cu-K_α radiation.

The hydrogen storage capacity was measured electrochemically. Test electrodes were prepared by pressing a mixture of alloy powder and copper powder (both <45 μm, weight ratio: 1:4) at 4 ton/cm^2. The electrodes were vacuum impregnated with 6 M KOH and cycled at 100 mA/g, charged for 4 h and discharged to a cut off potential of -0.6 V vs. Hg/HgO. Charge and discharge were both followed by a resting period of 30 min.

Information about phase diagrams is taken from Massalski [1] and X-ray diffraction data from JCPDS-International Centre for Diffraction Data (1997). X-ray data on $CaNi_2$

*Corresponding author.

0925-8388/99/$ – see front matter
PII: S0925-8388(99)00418-1

were not available. Instead data on $MgCu_2$ was used with appropriate fitting of the unit cell size. Values for the relative peak intensity were taken unchanged from the $MgCu_2$ data. Calculations of 2θ values were performed with the program REFBASE.

3. Results and discussion

3.1. Electrochemical capacities

In all cases the electrodes were easily activated. The maximum capacity was reached within the first or second cycle (except for $CaNi_4Sn$ with a negligible capacity even after 60 cycles). The electrochemical capacities ranged from 39 to 390 mAh/g, but none of the substitutions increased the cycling stability to any significant extent. Fig. 1 shows the capacity of the first 10 cycles of the cobalt substituted alloys. Capacities of all the alloys and some information on the capacity decay are summarized in Table 1. It appears that the cycleability is poor in all cases.

3.2. X-ray diffraction

All alloys were examined by X-ray diffraction, but due to limited space only some examples of X-ray patterns are shown hereafter. The diffraction patterns revealed that only in a few cases the hexagonal $CaCu_5$ structure of a true AB_5 alloy was preserved. To find an explanation to this the substitution elements are divided into three groups based on which intermetallics they form with calcium.

3.2.1. Group 1: Cu and Zn

These metals are able to replace Ni completely in $CaNi_5$ thus forming the iso-structural compounds $CaCu_5$ or $CaZn_5$ respectively. In this group, as expected, the hexagonal structure was preserved for $x=0.5$ and 1 for both Cu and Zn. The unit cell dimensions were increased slightly following the sequence $CaNi_5<CaNi_{5-x}Cu_x<CaNi_{5-x}Zn_x$ as well as for increasing x from 0.5 to 1 in $CaNi_{5-x}M_x$. This is in perfect agreement with the fact that the unit cell dimensions increases following the sequence $CaNi_5<CaCu_5<CaZn_5$.

Table 1
Electrochemical capacities of the alloys with some brief information on cycleability

Alloy (overall formula)	Max. capacity (mAh/g)	$n_{>50\%}$ [a]	$n_{>100\ mAh/g}$ [b]
$CaNi_5$ [c]	369	4	7
$CaNi_5$ [d]	388	3	6
$CaNi_{4.5}Al_{0.5}$	207	1	1
$CaNi_4Al$	61	3	0
$CaNi_{4.5}Cr_{0.5}$	175	1	1
$CaNi_4Cr$	93	2	0
$CaNi_{4.5}Mn_{0.5}$	195	3	3
$CaNi_4Mn$	174	1	2
$CaNi_{4.5}Fe_{0.5}$	158	1	1
$CaNi_4Fe$	54	4	0
$CaNi_{4.5}Co_{0.5}$	238	2	2
$CaNi_4Co$	185	1	1
$CaNi_{4.5}Cu_{0.5}$	384	3	5
$CaNi_4Cu$	371	4	8
$CaNi_{4.5}Zn_{0.5}$	388	3	6
$CaNi_4Zn$	387	3	10
$CaNi_{4.5}Sn_{0.5}$	232	5	6
$CaNi_4Sn$	39	–	0
$CaNi_{4.5}Mg_{0.5}$	390	4	11
$CaNi_4Mg$	321	3	10

[a] $n_{>50\%}$ is the number of cycles with more than 50% of the maximum capacity preserved.
[b] $n_{>100\ mAh/g}$ is the number of cycles with a capacity of more than 100 mAh/g.
[c] A commercial alloy from Ergenics Inc.
[d] An alloy prepared by mechanical alloying.

3.2.2. Group 2: Cr, Mn, Fe and Co

These metals are not known to form any binary intermetallics with calcium. In this group no AB_5 phases were seen. Instead the compounds Ca_2Ni_7, $CaNi_3$ or $CaNi_2$

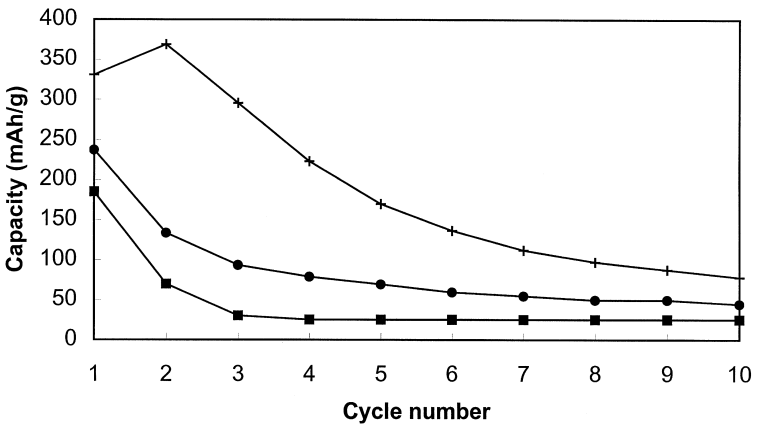

Fig. 1. Electrochemical capacity curves for the alloys with the overall composition $CaNi_{4.5}Co_{0.5}$ (circles) and $CaNi_4Co$ (squares). $CaNi_5$ (crosses) is included for comparison.

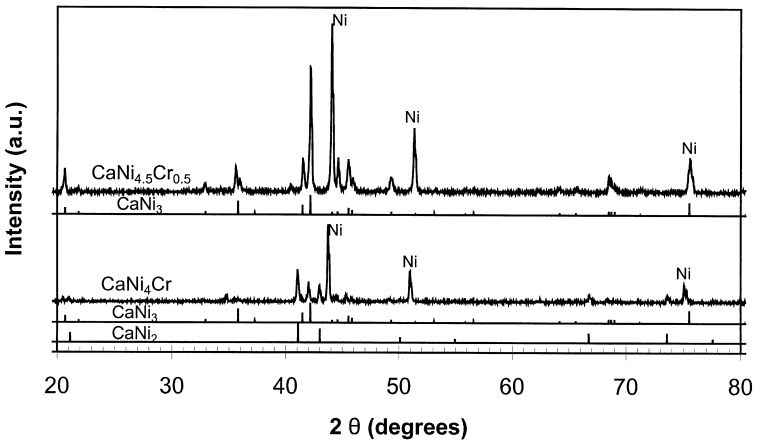

Fig. 2. X-ray diffraction patterns for the alloys with the overall composition $CaNi_{5-x}Cr_x$. The line patterns for $CaNi_3$ and $CaNi_2$ are included for comparison.

were formed together with a nickel-like phase represented by peaks of strong intensity. As an example the X-ray diffraction patterns for the chromium substituted alloys are shown in Fig. 2.

For all alloys with substitution elements from this group the X-ray patterns of the calcium–nickel phases had 2θ values in good agreement with the literature indicating a low impurity level. On the other hand, the 2θ values of the nickel phase were in most cases shifted towards lower values compared to pure nickel. This shift, which is indicating a larger unit cell size, increased when x increased from 0.5 to 1. The reason for the larger unit cell size is probably that atoms of the substitution element are dissolved in the phase thus imposing a strain. The cobalt substituted alloys were exceptions. For both alloys the position of the nickel phase peaks were very close to the values of pure nickel. This is attributed to similar metallic radii of the nickel and the cobalt atoms.

Table 2 provides an overview of the calcium–nickel phases formed with the different substitutions.

A few unidentified peaks in each X-ray pattern indicated that one or more other phases were present, but most of these were of low intensity. They could not be identified as pure elements or any binary intermetallic of the involved metals. The excess peaks are probably to be explained by ternary (or higher order) compounds of which no X-ray data are available. There were no signs of CaO which is expected to be formed in case of oxygen contamination in systems like this where calcium is the most electropositive element present.

The well known absence of binary intermetallic compounds of calcium and Cr, Mn, Fe or Co can be taken as evidence of poor affinity between Ca and these elements. This poor affinity explains why pure calcium–nickel compounds are formed instead of AB_5-phases. The remaining substitution elements must then mostly be dissolved in the nickel or nickel-like phase as described above.

3.2.3. Group 3: Al, Sn and Mg

These metals do form binary intermetallics with Ca, but not with the stoichiometry AM_5.

The case of Al-substitution is very similar to group 2 substitution. For $x=0.5$ a Ca_2Ni_7 pattern with high intensity was formed and for $x=1$ a $CaNi_2$ pattern of lower intensity was formed. A pronounced Ni phase was shifted markedly towards lower angles in both cases. No sign of binary Ca–Al compounds was seen, but traces of some Al–Ni compounds could not be excluded due to a number of smaller unidentified peaks.

The Sn substituted alloys contained AB_5 phases for both $x=0.5$ and $x=1$. The diffraction angles were shifted

Table 2
The Ca–Ni phases formed in alloys with the overall composition $CaNi_{5-x}M_x$

M=	Al		Cr		Mn		Fe		Co		Cu		Zn		Sn	
x=	0.5	1	0.5	1	0.5	1	0.5	1	0.5	1	0.5	1	0.5	1	0.5	1
$CaNi_5$											s[a]	s	s	s	s	s
Ca_2Ni_7	x								x							
$CaNi_3$			x	x	x	x	x	x		x						
$CaNi_2$		x		x		(x)[b]		x		(x)						

[a] s indicates distinctly shifted peaks with respect to $CaNi_5$.
[b] Brackets indicate a very small amount or uncertainty.

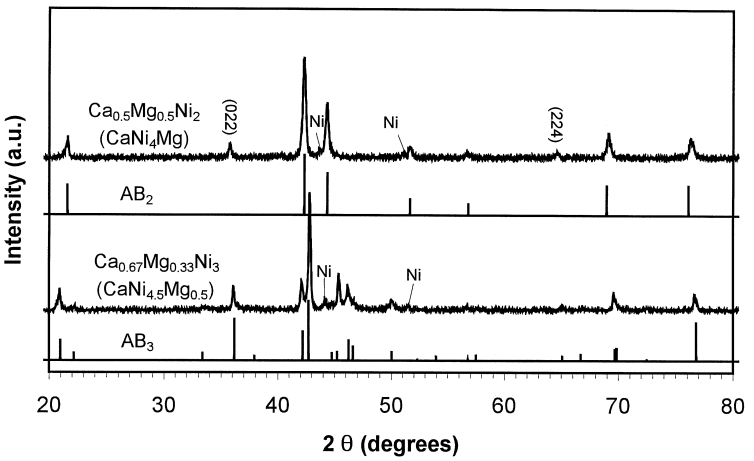

Fig. 3. X-ray diffraction patterns for the alloys with the overall composition $CaNi_{5-x}Mg_x$. The line patterns for AB_3 and AB_2 are calculated (see text).

towards lower values indicating a larger unit cell. This is consistent with the large Sn atoms. Anyhow, the shift was not more pronounced for $x=1$ than for $x=0.5$ (as for the Cu or Zn alloys). A reason for this could be that the maximum amount of Sn is reached (or passed) for $x=0.5$. Further addition of Sn only results in increased formation of other phases. Besides the AB_5 pattern a set of Ni peaks (with no shifting) and more than 20 other unidentified peaks were seen in both patterns. Moving from $x=0.5$ to $x=1$ resulted in a decrease of all peaks assigned to AB_5 while the unidentified peaks increased. In other words, the amount of AB_5 phase decreased while the unidentified phases increased with increasing Sn content. The Ni peaks remained practically constant. It was not possible to assign the other peaks with certainty to any binary Ca–Ni, Ca–Sn or Ni–Sn phase nor pure elements. A pattern of CaO due to some oxygen contamination was possible.

Mg is a typical A metal with a high hydrogen affinity. In this work Mg was attempted used as a B metal substitute in the AB_5 system. The reason for this is that it was expected to suit the B metal positions better than the A metal positions because Mg is smaller than Ca. A larger content of elements with affinity for hydrogen could enhance the storage capacity. The overall compositions of the alloys were $CaNi_{4.5}Mg_{0.5}$ and $CaNi_4Mg$ but the X-ray patterns revealed that Mg clearly enters Ca positions, see Fig. 3. The resulting compounds were then $Ca_{0.67}Mg_{0.33}Ni_3$ (AB_3) and $Ca_{0.5}Mg_{0.5}Ni_2$ (AB_2) respectively. It is evident that the Ca:Ni:Mg ratios are the same when the formulas are written this way. $CaNi_3$ and $CaNi_2$ are iso-structural with $PuNi_3$ and $MgCu_2$. Unit cells of these structures were fitted to the diffraction patterns of the Mg substituted alloys based on the values of 2θ. These data are included in Fig. 3. The relative peak intensities are taken from $CaNi_3$ and $MgCu_2$. The calculated patterns adapts well to the measured patterns. For the AB_2 unit cell, diffraction peaks were calculated for the planes (022) and (224), but these peaks are apparently not seen for $MgCu_2$. For $Ca_{0.5}Mg_{0.5}Ni_2$ However, distinct peaks are seen at the calculated positions and they are marked at the figure.

4. Conclusions

It can be concluded that $CaNi_5$ is much less tolerant towards B-metal substitution than $LaNi_5$, see Table 3. This fact makes it less possible that the problem with cycling stability of Ca-based hydride electrodes can be solved by substitutions. The present work also shows that Mg can substitute to some extent for Ca in $CaNi_3$ and $CaNi_2$. A similar substitution for Ca in $CaNi_5$ and perhaps also for La in lanthanide based AB_5 alloys are likely to be possible.

Acknowledgements

The authors wish to thank the Danish Environmental Protection Agency for the financial support of the present work.

Table 3
Maximum substitutions (x) with preservation of the $CaCu_5$ structure in $LaNi_{5-x}M_x$ and $CaNi_{5-x}M_x$

M=	Al	Cr	Mn	Fe	Co	Cu	Zn	Sn	Mg
$LaNi_{5-x}M_x$ [1,4]	1.3	<5	2.2	1.2	5	5	<5	<5	<5
$CaNi_{5-x}M_x$, this work [1]	<0.5	<0.5	<0.5	<0.5	<0.5	5	5	<0.5	<0.5

References

[1] T.B. Massalski, Binary Alloy Phase Diagrams, American Society for Metals, Metals Park, Ohio, 1986.
[2] G.D. Sandrock, J.J. Murray, M.L. Post, J.B. Taylor, Mater. Res. Bull. 17 (1982) 887.
[3] J.O Jensen, R.W. Berg, N.J. Bjerrum, to be published.
[4] A. Percheron-Guegan, M. Latroche, J.C. Achard, Y. Chabre, J. Bouet, J., in: P.D. Bennet, T. Sakai, (Eds.), Hydrogen and Metal Hydride Batteries, The Electrochemical Society, Pennington, New Jersey, USA, 1994, pp. 196–218.